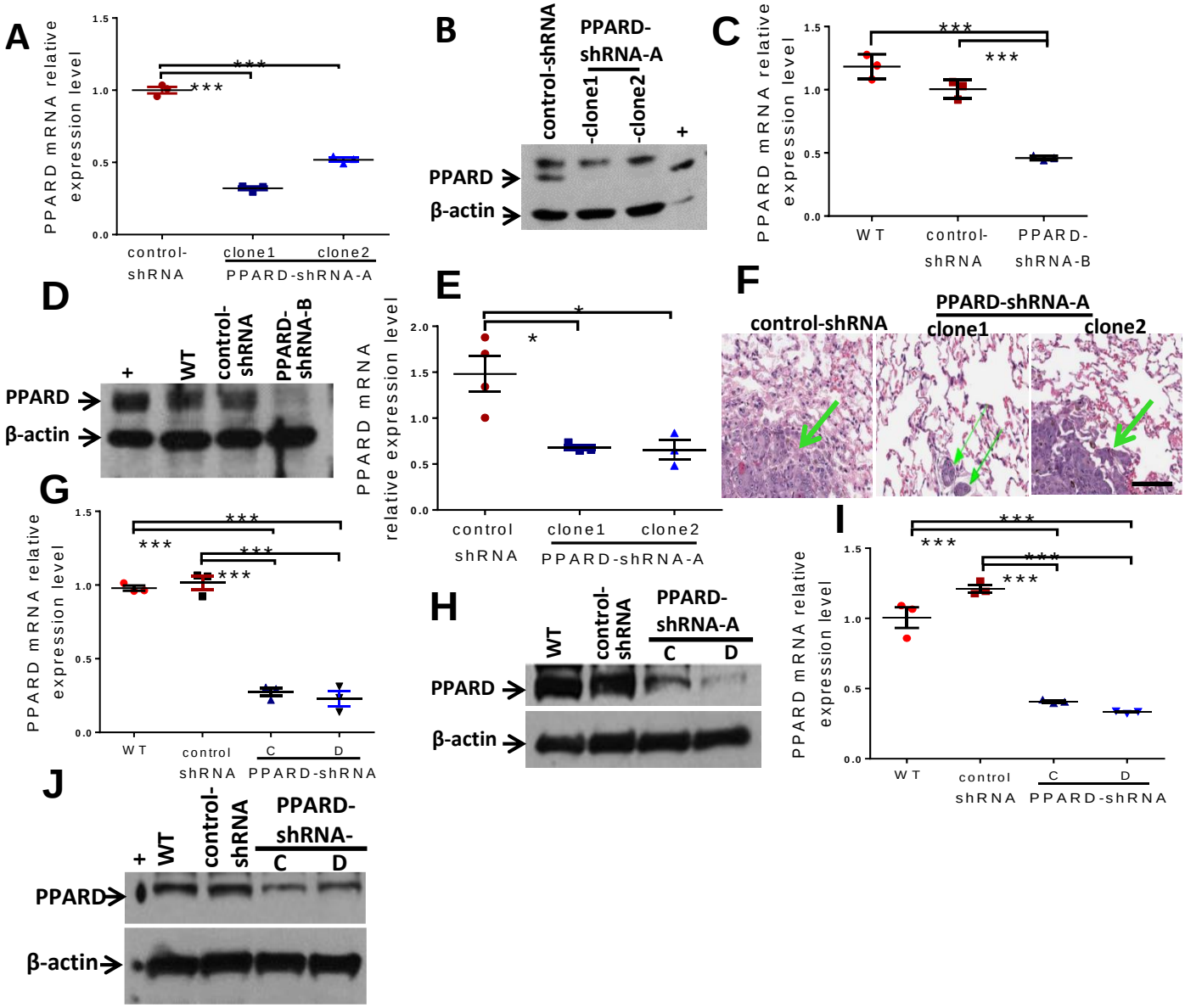

Supplemental Figure 1. PPARD downregulation by shRNA in B16-F10 and LLC cells. (A and B) PPARD expression levels in B16-F10 melanoma cells stably transfected with either PPARD-shRNA-A (PPARD-shRNA-A-clone1 or -clone2) or control-shRNA plasmid. **(A)** PPARD mRNA levels were measured using qRT-PCR. **(B)** PPARD protein levels were measured using Western blot analysis. **(C-D)** PPARD expression levels in LLC-GFP WT cells or LLC-GFP cells stably transfected with either a PPARD-shRNA-B (PPARD-shRNA) or a control-shRNA plasmid. **(C)** PPARD mRNA levels were measured using qRT-PCR. **(D)** PPARD protein levels were measured using Western blot analysis. **(E-F)** PPARD mRNA expression levels of lung metastases **(E)** and representative photomicrographs of hematoxylin and eosin-stained sections of lung metastases **(F)** for the lungs as shown in Figure **1, A and B**. Arrows indicate lung tumor foci. Scale bar: 100μm. **(G and H)** PPARD expression levels in melanoma B16-F10 WT or B16-F10 cells stably transduced with either PPARD-shRNA (PPARD-shRNA-C or D) or control-shRNA lentivirus. **(G)** PPARD mRNA levels were measured using qRT-PCR. **(H)** PPARD protein levels were measured using Western blot analysis. **(I and J)** PPARD expression levels in LLC-GFP WT cells or LLC-GFP cells stably transduced with either a PPARD-shRNA-C or -D or a control-shRNA lentivirus. **(I)** PPARD mRNA levels were measured using qRT-PCR. **(J)** PPARD protein levels were measured using Western blot analysis. **+:** positive control of PPARD was the lysate of mouse intestinal epithelial cells with PPARD overexpression. Values are means ± SDs for **A**,**C**,**E**, **G** and **I**. **P* < 0.01; ****P* < 0.0001 [one-way (**A**, **C** and **E**) or two way (**G** and **I**) ANOVA]. All data are representative of 3 independent experiments.

sFigure 2 **Zuo X, *et al.***

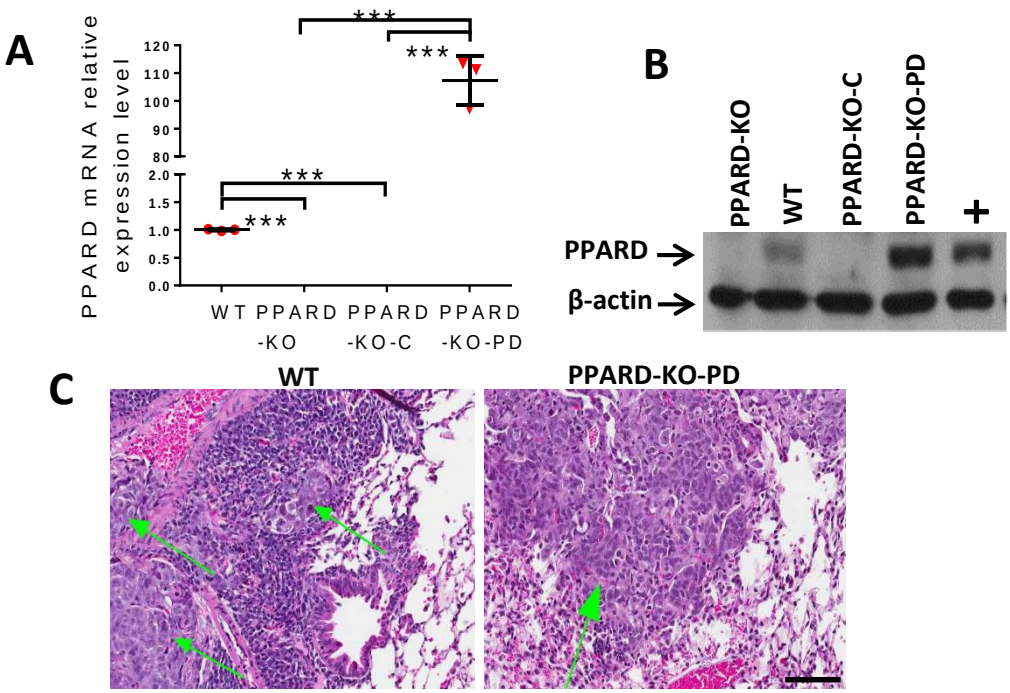

Supplemental Figure 2. PPARD genetic deletion and reconstitution in HCT-116 colon cancer cells and formation of lung metastases in immunodeficient mice. (A) PPARD mRNA expression levels were measured by q-RT-PCR. **(B)** PPARD protein expression levels were measured by Western blot analysis. **+:** positive control of the lysate of PPARD vector transfected HCT116 cells. **(C)** Representative photomicrographs of hematoxylin and eosin-stained sections of lung metastases formed 6 weeks after tail vein injection of HCT116 parental (WT), or PPARD-KO-PD cells. Arrows indicate lung tumor foci. Scale bar: 100μm. Values are means ± SDs. ***P < 0.0001 (two-way ANOVA). All data are representative of 3 independent experiments.

sFigure 3 **Zuo X, *et al.***

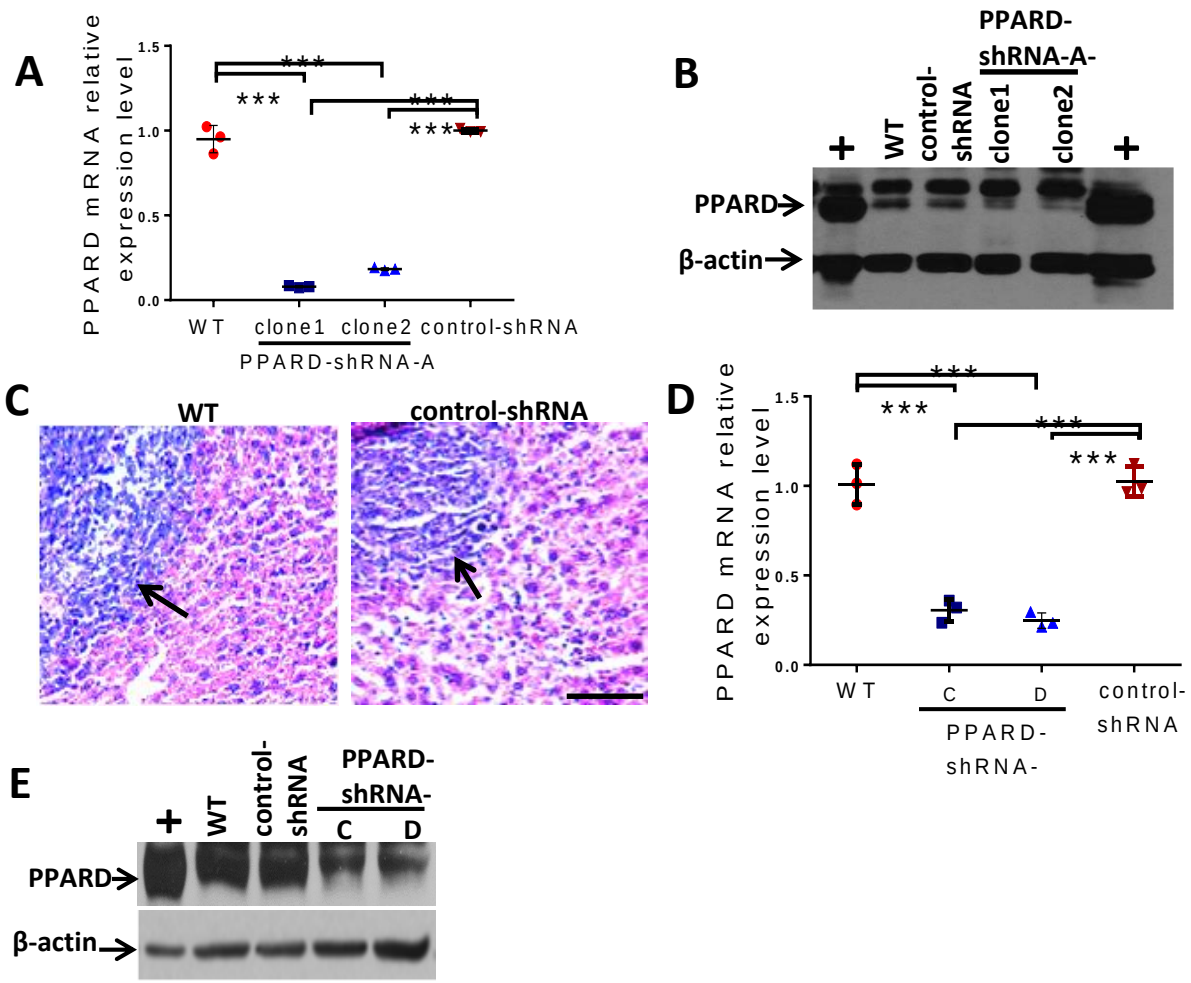

Supplemental Figure 3. PPARD downregulation in Panc-02 and 4T1 cancer cells. (A) PPARD mRNA expression levels, as measured by qRT-PCR, in WT Panc-02 cells and Panc-02 cells stably transfected with PPARD-shRNA-A (PPARD-shRNA-A-clone1 or -clone2) or control shRNA plasmid. **(B)** PPARD protein expression levels, as measured by Western blot analysis, in the cells described in panel **A**. **(C)** Representative photomicrographs of hematoxylin and eosin-stained sections of liver metastases of Panc-02 WT cells or Panc-02 cells stably transfected with control shRNA plasmid. Arrows indicate liver tumor foci. Scale bar: 100μm. **(D)** PPARD mRNA expression levels, as measured by qRT-PCR in WT 4T1 cells and 4T1 cells stably transduced with PPARD-shRNA-C or -D lentivirus or control shRNA lentivirus. **(E)** PPARD protein expression levels, as measured by Western blot analysis, in the cells described in panel **D**. **+:** positive control of PPARD was the lysate of mouse intestinal epithelial cells with PPARD overexpression. Values are means ± SDs for **A** and **D**. ***$P < 0.0001$ (two-way ANOVA). All data are representative of 3 independent experiments.

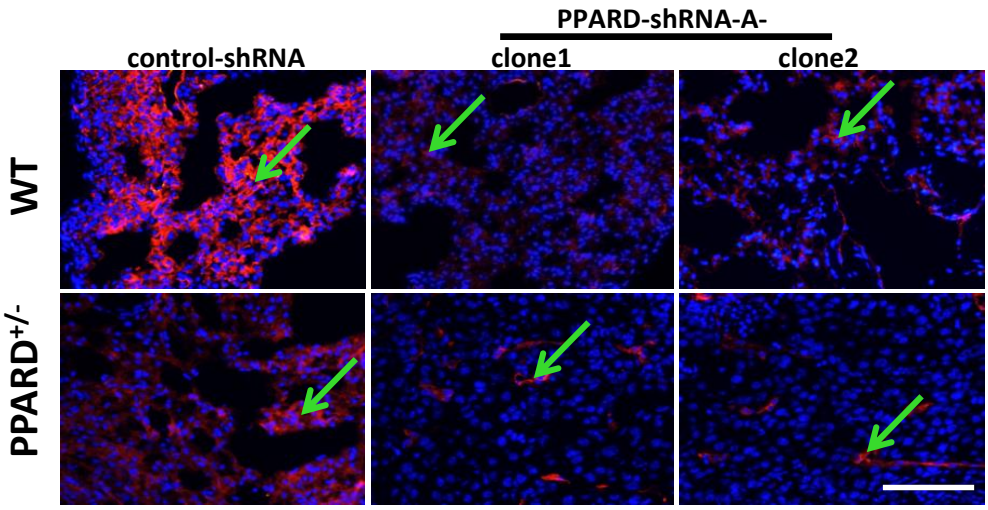

Supplementary Figure 4. PPARD downregulations in cancer cells inhibits tumor angiogenesis in vivo. Lung metastases formed 3 weeks after tail-vein injection of B16-F10 cells stably transfected with PPARD-shRNA-A (PPARD-shRNA-A-clone1 or -clone2), or control-shRNA into C57BL/6 WT or PPARD$^{+/-}$ mice. The lung tissues with metastases were then harvested in optimum cutting temperature compound and subjected to immunofluorescence staining for CD31 to visualize blood vessel formation. Arrows indicate tumor blood vessels (stained red). Scale bar: 100μm.

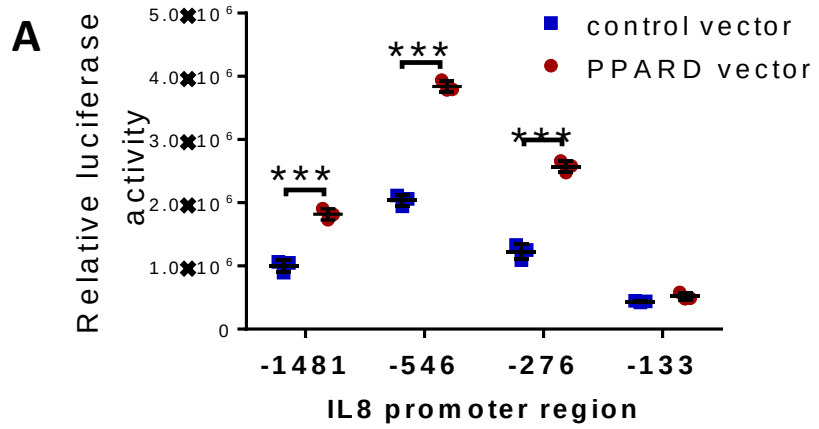

Supplemental Figure 5. Effects of PPARD expression in LoVo cancer cells on IL8 promoter activity. (A) LoVo cells transfected with PPARD vector or control vector were transiently transfected with PGL4.16 luciferase reporter vector containing the IL8 promoter regions of −1481 to +50 bp (−1481), –546 to +50 bp (–546), –276 +50 bp (–276) and –133 to +50 bp (–133) and with pSV-β-galactosidase vector. Luciferase activity was measured 24h later and normalized for β-galactosidase activity. Results are means ± SDs. ***$P < 0.0001$ (two-way ANOVA). Data are representative of 3 independent experiments.

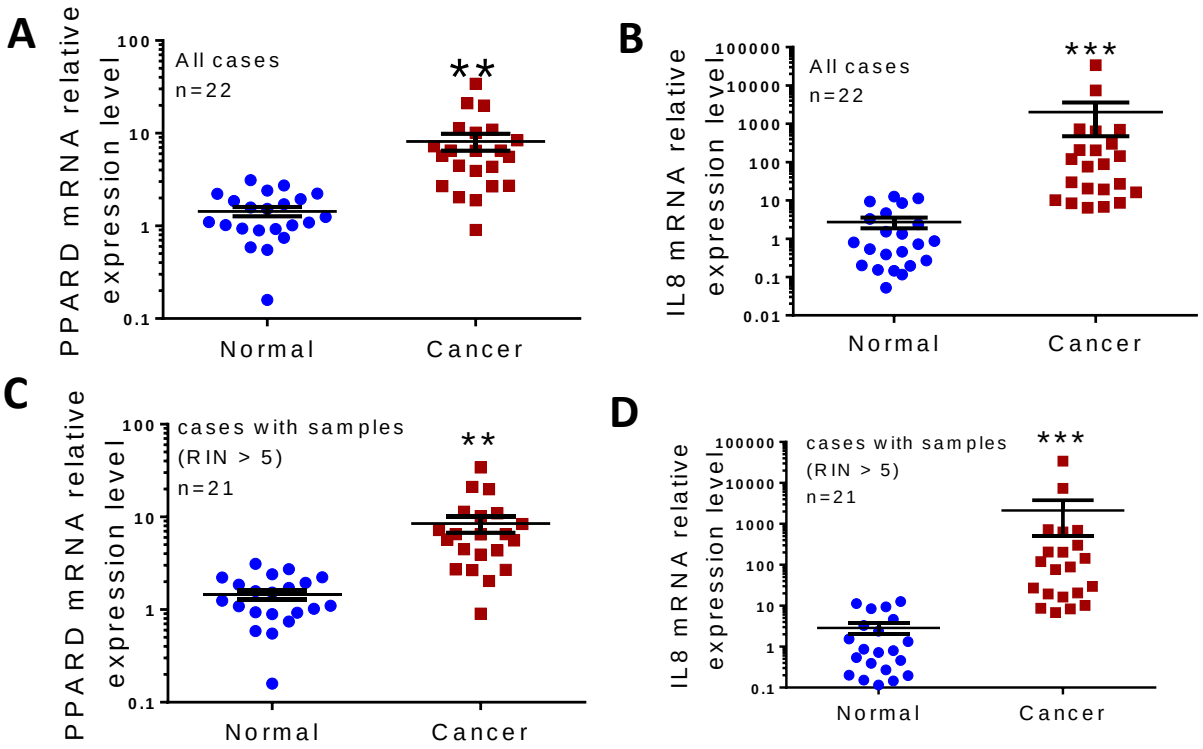

Supplemental Figure 6. PPARD and IL8 expression levels in human colon cancers. (A-D) Comparative analyses of PPARD and IL8 mRNA levels in samples of normal mucosa and cancerous mucosa from patients with stage III colon cancer, in relation to RNA integrity number (RIN) measurements of RNA quality. **(A and B)** Scatter plots of PPARD mRNA levels **(A)** and IL-8 mRNA levels **(B)** in paired normal and cancerous mucosa samples (n = 22). Each dot represents the mean measurement for an individual. **(C and D)** Scatter plots of the PPARD and IL8 mRNA levels presented in panels **A** and **B**, excluding results from samples that had RIN < 5 (n = 21). Each dot represents the mean measurement for an individual. Values are means ± SEM. ** $P < 0.001$, ***$P < 0.0001$ (paired *t*-test).

sFigure 7 **Zuo X, *et al.***

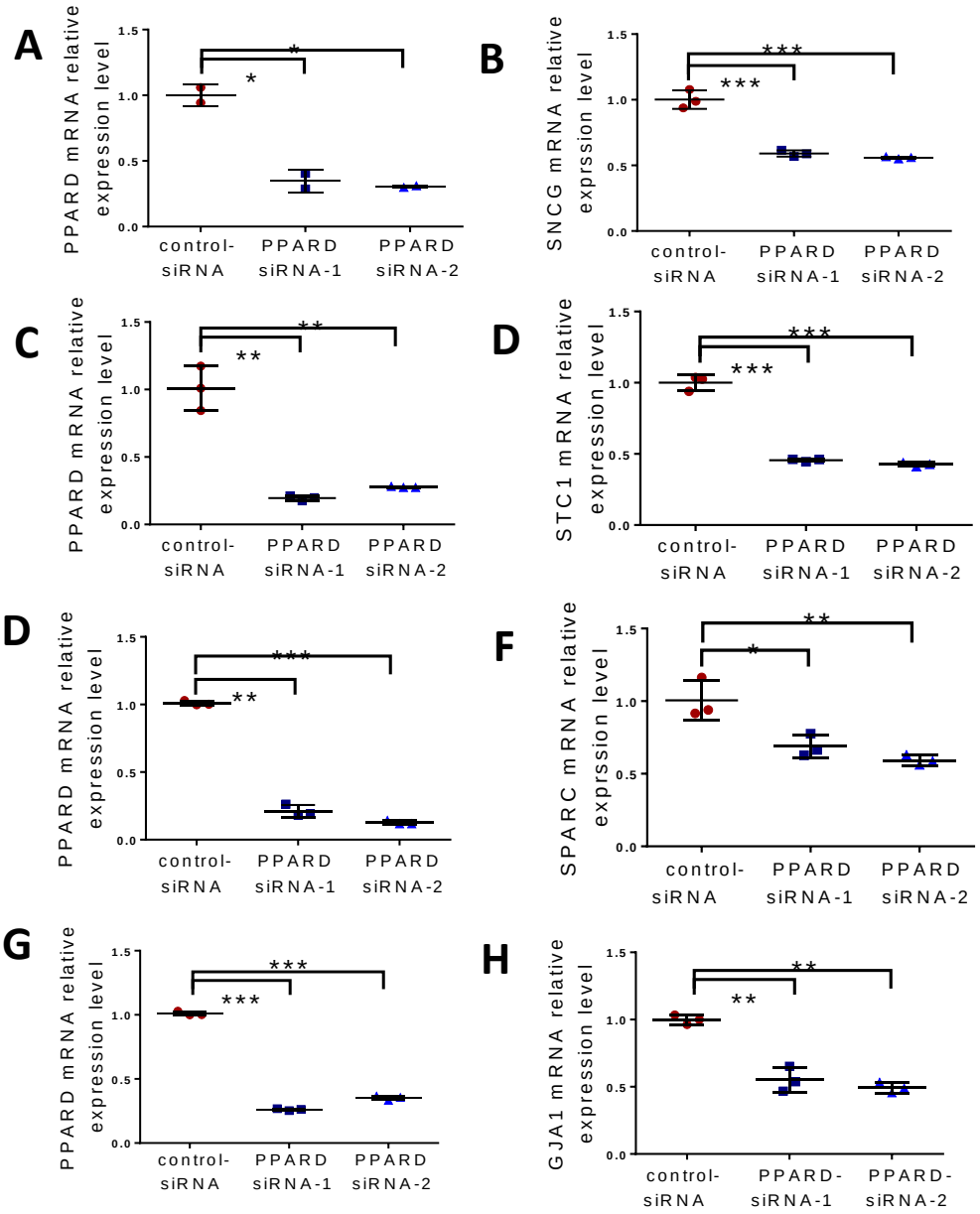

Supplemental Figure 7. **PPARD downregulation inhibits SNCG, STC1, GJA1 and SPARC expressions in cancer cells.** SW620 **(A and B),** HeyA8 ovarian cancer cells **(C and D),** SW480 **(E and F),** and LoVo **(G and H)** were transfected with PPARD siRNAs (PPARD-siRNA-1 or -2) or control siRNA for 48 h and then harvested for analysis of mRNA expression levels of PPARD and other indicated genes as measured by qRT-PCR. Values are means ± SDs. **P* < 0.01; ***P* < 0.001; ****P* < 0.0001 (one-way ANOVA). Data are representative of 3 independent experiments.

sFigure 8

Zuo X, *et al.*

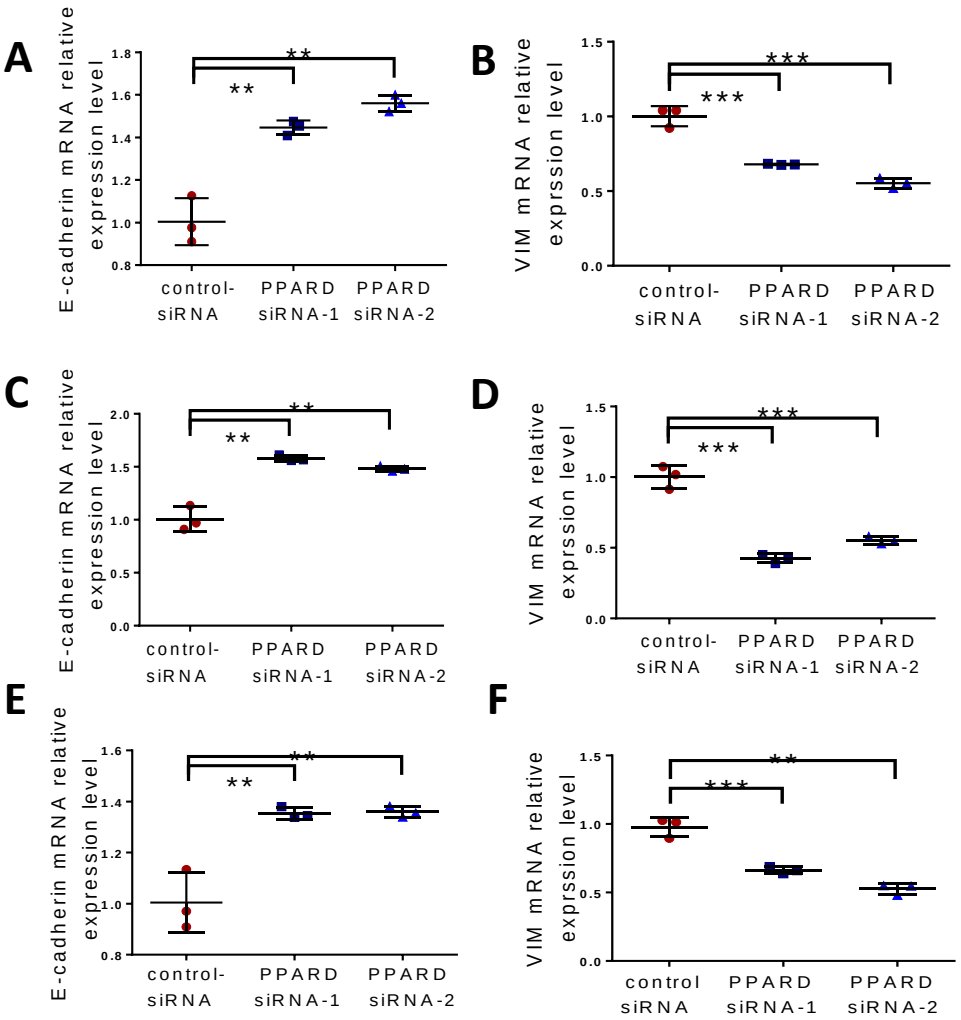

Supplemental Figure 8. PPARD downregulation upregulated E-cadherin and inhibited vimentin expressions in colon cancer cell lines other than HCT116. SW480 **(A and B)**, SW620 **(C and D)**, and LoVo **(E and F)** cells were transfected with 2 different specific PPARD siRNAs (PPARD-siRNA-1 or -2) or control-siRNA for 48 h and then harvested for analysis of mRNA expression levels of E-cadherin, and vimentin (VIM) genes as measured by qRT-PCR. Values are means ± SDs. ***P* < 0.001; ****P* < 0.0001 (one-way ANOVA). Data are representative of 3 independent experiments.

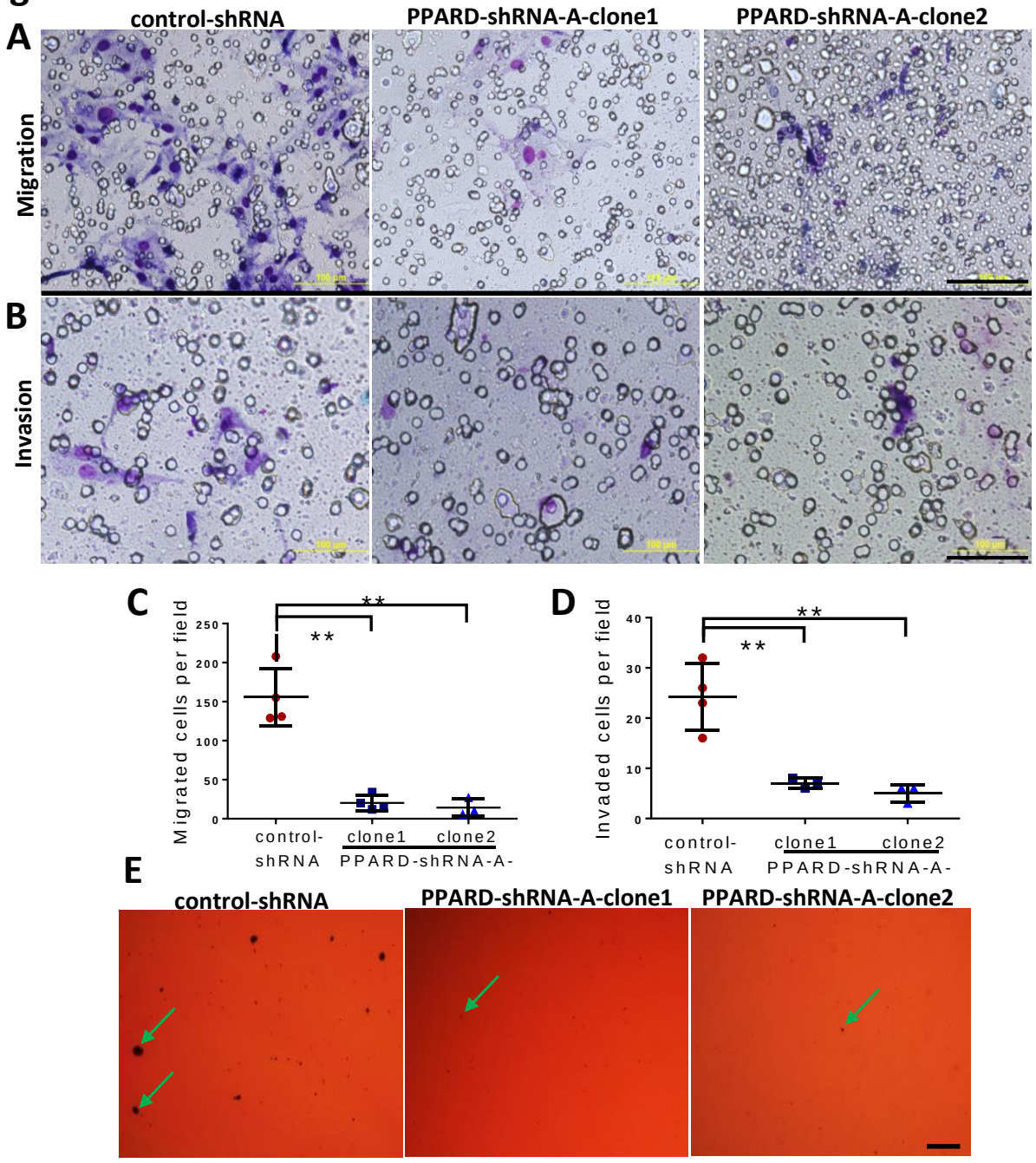

Supplemental Figure 9. PPARD downregulation inhibits the migration, invasion, and anchorage-independent growth of B16F10 melanoma cells. (A-D) PPARD downregulation inhibits migration and invasion of B16-F10 cells stably transfected with control-shRNA or PPARD-shRNA (PPARD-shRNA-A-clone1 or -clone2). **(A and B)** Representative photomicrographs of migrated **(A)** or invaded **(B)** B16-F10 cells. **(C and D)** Migrated cells **(C)** and invaded cells **(D)** in at least 4 random individual fields per insert membrane were counted. Values are means ± SDs. **(E)** PPARD downregulation inhibits anchorage-independent growth of B16-F10 cells stably transfected with control-shRNA or PPARD-shRNA (PPARD-shRNA-clone1 or -clone2). Representative photomicrographs of soft agar colonies of the indicated cells. Green arrows indicate formed colonies. Scale bars for panels **A** and **B**: 100µm; for panel **E**: 1mm. $^{**}P < 0.001$ (one-way ANOVA). Data are representative of 3 independent experiments.

sFigure 10 **Zuo X, *et al.***

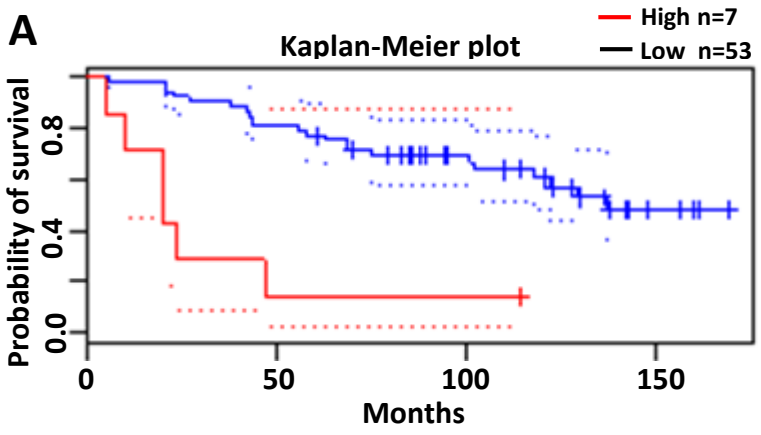

DATASET	GSE1378
CANCER_TYPE	Breast cancer
SUBTYPE	
N	60
ENDPOINT	Relapse Free Survival
COHORT	MGH (1987-2000)
ARRAY TYPE	Arcturus 22k
CONTRIBUTOR	Ma
MINIMUM P-VALUE	0.000009
CORRECTED P-VALUE	0.000409
ln(HR$_{high}$ / HR$_{low}$)	1.88
COX P-VALUE	0.000267
ln(HR)	0.71
HR [95% CI]	2.02 [1.39 - 2.96]

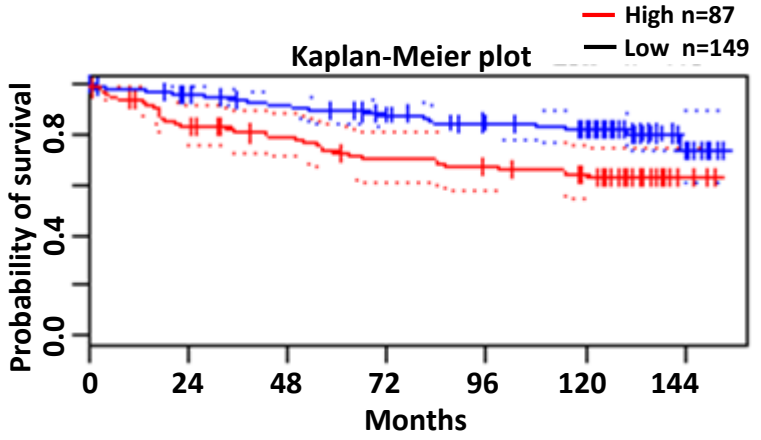

DATASET	GSE3494-GPL96
CANCER_TYPE	Breast cancer
N	236
ENDPOINT	Disease Specific Survival
COHORT	Uppsala (1987-1989)
ARRAY TYPE	HG-U133A
CONTRIBUTOR	Miller
MINIMUM P-VALUE	0.001461
CORRECTED P-VALUE	0.034963
ln(HR$_{high}$ / HR$_{low}$)	0.84
COX P-VALUE	0.005177
ln(HR)	1.07
HR [95% CI]	2.93 [1.38 - 6.22]

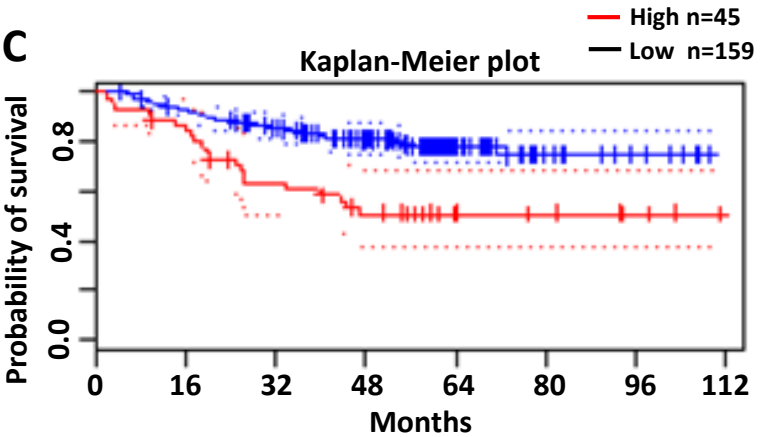

DATASET	GSE31210
CANCER_TYPE	Lung cancer
SUBTYPE	Adenocarcinoma
N	204
ENDPOINT	Relapse Free Survival
PERIOD	Days
COHORT	NCCRI
ARRAY TYPE	HG-U133_Plus_2
CONTRIBUTOR	Okayama
MINIMUM P-VALUE	0.000216
CORRECTED P-VALUE	0.006886
ln(HR$_{high}$ / HR$_{low}$)	0.99
COX P-VALUE	0.013715
ln(HR)	0.89
HR [95% CI]	2.45 [1.20 - 4.98]

Supplemental Figure 10. The relationship between PPARD expression levels and cancer patient survival. (A-C) Kaplan-Meier survival estimates of relapse-free survival **(A** and **C)** and disease-specific survival **(B)** as a function of high versus low PPARD expression in the tumors of the indicated patient cohorts based on analyses of data sets in the PrognoScan database.

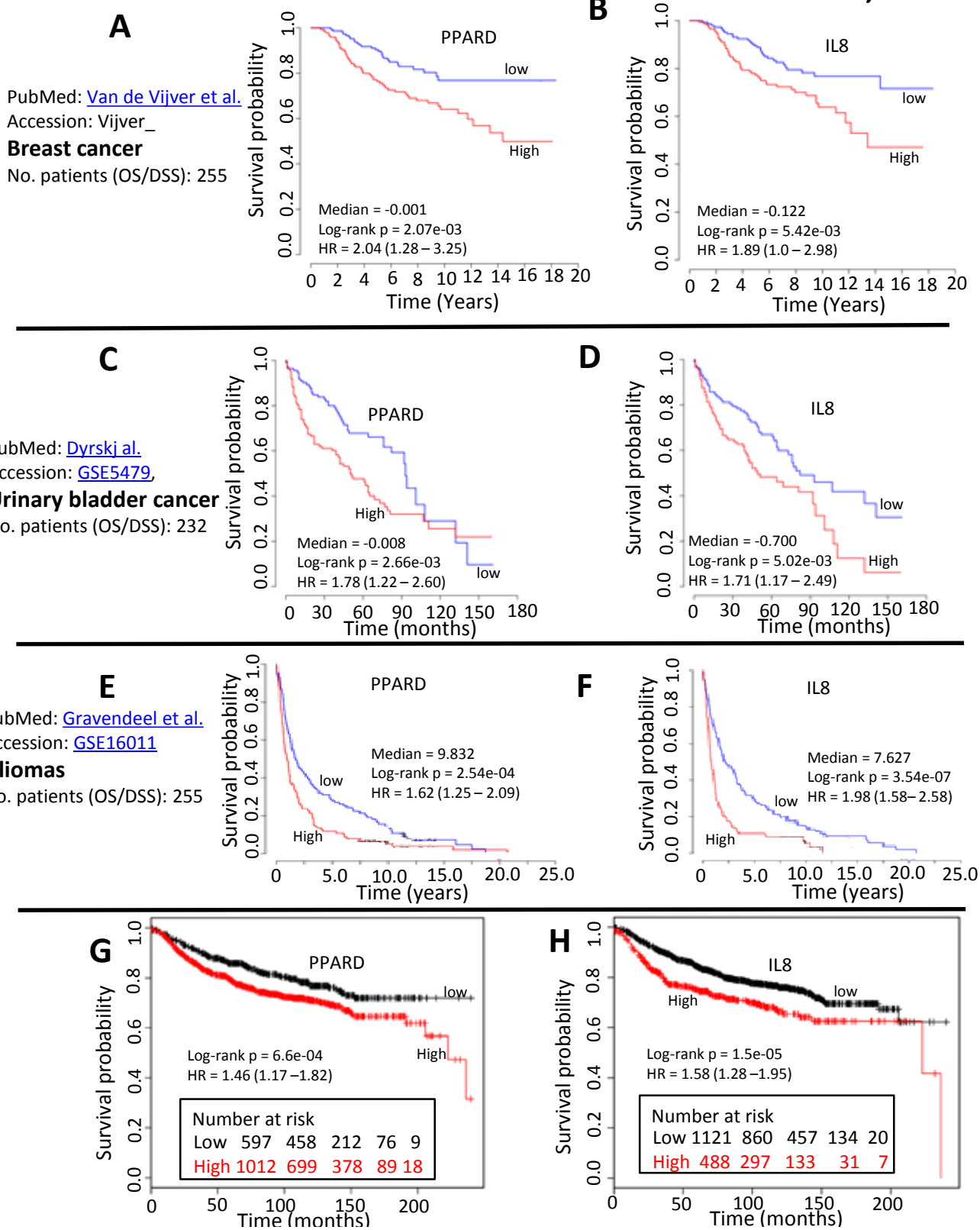

Supplemental Figure 11. **The relationship between PPARD and IL8 expression levels and cancer patient survival. (A-F)** Kaplan-Meier survival estimates of overall survival for cohort of breast cancer (**A** and **B**), urinary bladder cancer (**C** and **D**) and gliomas (**E** and **F**) as a function of high versus low PPARD or IL8 expression in the indicated cancer patient cohorts based on their data set analyses in the PRECOG public database portal. **(G** and **H)** Kaplan-Meier analyses of distant metastasis free survival as a function of high versus low PPARD or IL8 expression of 1609 breast cancer patients included in the KMPlot public database portal.

SUPPLEMENTAL METHODS

Cell lines and culture conditions. The human colon cancer cell lines HCT116, LoVo, SW480, and SW620 and the mouse breast cancer cell line 4T1 were from American Type Culture Collection; human umbilical vein endothelial cells (HUVECs), from Cambrex; mouse Lewis lung cells expressing green fluorescent protein (LLC-GFP cells), from Dr. Dipak Panigrahy (Harvard Medical School, Boston Children's Hospital, Boston, MA); mouse B16-F10 melanoma cells from Dr. Isaiah J. Fidler (The University of Texas MD Anderson Cancer Center, Houston, TX), and Panc-02 pancreatic cancer cells from Dr. Keping Xie (The University of Texas MD Anderson Cancer Center); HCT116 parental and peroxisome proliferator–activated receptor-δ (PPARD)-knockout (KO) cells, from Dr. Bert Vogelstein (Johns Hopkins University, Baltimore, MD); and Hey8A cells, from Dr. Gordon B. Mills (The University of Texas MD Anderson Cancer Center, Houston, TX).

SW480, LoVo, HCT116, and PPARD-KO cells were maintained in McCoy's medium supplemented with 10% fetal bovine serum (FBS; VWR International). 4T1, SW620 and Hey8A cells were maintained in RPMI medium supplemented with 10% FBS. Panc-02, B16-F10 and LLC-GFP cells were maintained in Dulbecco's modified Eagle's medium (DMEM; 4.5 g/L glucose for Panc-02 and B16-F10 cells and low glucose for LLC-GFP cells) supplemented with 10% FBS and 2 mM L-glutamine, penicillin, and streptomycin (Life Technologies). Growth factor-reduced Matrigel basement membrane matrix was from BD Biosciences.

Clinical samples. Samples of paired cancerous and normal colonic mucosa collected from 2003 through 2006 were obtained from a tumor tissue repository at MD Anderson Cancer Center with

Institutional Review Board approval. All tissue samples were placed in RNAlater, maintained at 4°C overnight, and then stored at -80°C until laboratory analyses.

For the immunohistochemical staining studies, samples from patients with stage II-IV colon cancer who underwent surgical resection at MD Anderson Cancer Center from July 2001 through July 2009 were identified. Blocks were selected, and a tissue microarray was constructed using 2 cores from tumor-bearing regions identified by hematoxylin and eosin staining and 1 core from normal colon tissue identified in a separate surgical block. All patients had provided consent for their tissues to be used in future research, and this retrospective study was approved by MD Anderson Cancer Center's Institutional Review Board. Patients were followed for recurrence and death, and the median follow-up time was 6.6 years.

Generation of cell lines stably overexpressing PPARD. The full length of the human PPARD cDNA was subcloned into a pcDNA3.1 plasmid (Life Technologies). HCT116 cells and HCT116 cells with PPARD KO (PPARD-KO cells) were transfected with pcDNA3.1 vector containing PPARD cDNA (PPARD vector) or pcDNA3.1 empty vector (control vector) and grown in selective medium containing hygromycin B (Roche Diagnostics; 400 μg/mL for HCT116 cells and 100 μg/mL for PPARD-KO cells). Stably transfected clones of PPARD vector-transfected and control vector-transfected cells were isolated and expanded.

Mouse orthotopic metastasis model. Panc-02 orthotopic model: Viable wild-type (WT) Panc-02 cells or Panc-02 cells stably transfected with PPARD-shRNA-A (PPARD-shRNA-A-clone1 or -clone2) or control-shRNA (1×10^5 in 50 μL of equal amounts of DMEM with high glucose and Matrigel) were prepared and injected into the pancreases of 6- to 8-week-old C57/B6 mice. Four

weeks after injection, the mice were killed by CO_2 asphyxiation, the pancreas tumors were measured and weighed, the liver tumors were counted, and images of the pancreases and livers were captured. Tumor volume was calculated as (length × width^2)/2 as described previously(1).

4T1 orthotopic model: Ten-week-old BALB/c mice were purchased from Charles River Laboratories. The mice were monitored for 2 weeks before being randomly assigned to receive injection with WT 4T1 cells or 4T1 cells stably transducted with control shRNA, PPARD-shRNA-C, or PPARD-shRNA-D lentivirus. Each mouse was injected with 1×10^4 cells in 100 µl of Hank's balanced salt solution into the fourth mammary fat pad. Injection sites were monitored for primary tumor growth. Mammary tumors were removed once they reached 1 cm in greatest diameter. Two weeks after the primary mammary tumors were removed, the mice underwent chest computed tomography for lung imaging. For lung CT imaging, the mice were anesthetized with isoflurane and intubated using a 22g 1inch catheter. A CT acquisition was acquired at 60kV and 4mA for 20 seconds. During the CT a breath hold was performed for 20 seconds to aid in the visualization of the lungs at full inspiration. The mice were extubated and placed in a warm cage until fully recovered. Mice were humanely killed on the following day and the lung surface tumors were then counted and photographed.

Liver metastasis xenograft formation by human colon cancer cells in immunodeficient mice and treatment with PPARD agonist GW0742. Six- to eight-week-old female athymic nude mice were purchased from MD Anderson Cancer Center's Animal Experimental Radiation Oncology Animal Facility and maintained under specific pathogen-free conditions. HCT-116 cells (1.0×10^6) stably transfected with a luciferase reporter gene via lentivirus (HCT-116-Luc cells) (2) or PPARD-KO cells (1.0×10^6) in 50 µL of equal amounts of DMEM with high glucose

and Matrigel were injected into mice's spleens (10-12 mice per group). Mice were fed either a standard laboratory diet (Harland Teklad 2019 chow diet) or the standard diet plus GW0742 at a concentration of 1 mg/kg (Teklad Custom Diet, TD10961) starting the day after cell injection. Liver metastasis growth in the mice injected with HCT116-Luc cells was monitored using bioluminescent imaging beginning 2 weeks after injection. Animals were anesthetized with a 2% isoflurane/oxygen mixture and injected intraperitoneally with 15 mg/mL D-luciferin potassium salt in phosphate-buffered saline (PBS; 150 mg/kg) and then placed onto a warmed stage inside a light-tight chamber. Imaging was done 12 min after the injection of D-luciferin. The level of luciferase expression was assessed using a bioluminescent IVIS imaging system (Xenogen Corp.). Four weeks after injection, the mice were killed by CO_2 asphyxiation, the liver tumors were weighed, and the livers were photographed. Tumor specimens from each group were snap frozen, preserved in RNAlater (Life Technologies), or fixed in formalin.

Total RNA extraction and qPCR. Total RNA was isolated using TRI reagent (Molecular Research Center Inc.). RNA samples were quantified, and 500 ng of total RNA was reverse-transcribed into cDNA using the iScript kit (Bio-Rad Laboratories). qPCR analyses were performed using a 7300 real-time PCR system (Applied Biosystems) as described previously(3). The relative RNA expression level was calculated using a comparative C_t method (ddC_t)(4).

Western blot analysis. Cells were homogenized in lysis buffer (0.5% Nonidet P-40, 20 mM 3-[N-morpholino] propanesulfonic acid [pH 7.0], 2 mM ethylene glycol tetraacetic acid, 5 mM ethylenediaminetetraacetic acid, 30 mM sodium fluoride, 40 mM β-glycerophosphate, 2 mM sodium orthovanadate, 1 mM phenylmethylsulfonyl fluoride, and 1× complete protease inhibitor

cocktail [Roche Applied Science]). Fifty-microgram samples of each protein were separated onto 7.5~10% sodium dodecyl sulfate polyacrylamide gel. After electrophoresis, the proteins were transferred to a nitrocellulose membrane. The membranes were blocked with 5% milk for 2 h at room temperature and hybridized with anti-human PPARD (Santa Cruz Biotechnologies, sc-7197), anti-mouse PPARD (Abcam, ab8937), anti-vimentin (BD Biosciences, #550513), anti-E-cadherin (BD Biosciences, #610182), anti-ZEB1 (Sigma, HPA027524), anti-SNAIL (Santa Cruz Biotechnologies, sc-10433), anti-TWIST (Santa Cruz Biotechnologies, sc-15393), or anti-GRHL2 (Sigma, SAB1408000) antibodies at 4°C overnight. Then, the blots were hybridized with the secondary antibody for 1 h at room temperature. The blots were analyzed using enhanced chemiluminescence (GE Healthcare).

CD31 immunohistochemical staining and immunofluorescence staining.

Immunohistochemical staining and immunofluorescence staining for the endothelial cell marker CD31 was performed on freshly cut frozen sections of optimum cutting temperature compound-embedded tissue using methods similar to those described previously(5-8). Briefly, sections were fixed in cold acetone for 15 min, washed with PBS, blocked with 4% fish gel, and incubated with rat monoclonal anti-mouse CD31 (BD Biosciences Pharmingen) overnight at 4°C. For CD31 immunohistochemistry, sections were washed with PBS, incubated with horseradish peroxidase–conjugated goat anti-rat immunoglobulin G (Jackson ImmunoResearch Laboratories) for 1 h, stained with Ferangi Blue Chromogen (Biocare Medical), and counterstained with Gil's hematoxylin (BioGenex Laboratories). For CD31 immunofluorescence staining, sections were washed with PBS and incubated with Alexa Fluor 488-conjugated goat anti–rabbit immunoglobulin G (Molecular Probes) for 1 h. Nuclei were stained with 4',6-diamidino-2-

phenylindole (DAKO). The microvessel density (MVD) marker CD31 was determined by performing a quantitative assessment of at least 3 random fields per tumor at ×200 magnification.

Human angiogenesis antibody array assay. An angiogenesis antibody array assay (Panomics, Inc.) was used to identify possible factors through which PPARD expression in cancer cells enhances tumor angiogenesis. HCT116 control vector–transfected and PPARD vector–transfected cells were cultured in serum-free medium for 48 h, and the culture media (conditioned media) were then separately collected. The assay involved the use of an array membrane on which specific antibodies to 19 angiogenesis-related factors were immobilized. An equal volume of each conditioned medium was incubated with a separate angiogenesis antibody array membrane for 2 h at room temperature. Next, the membranes were incubated with biotin-labeled secondary antibody solution for 2 h and processed using the streptavidin-horseradish peroxidase chemiluminescence method to detect protein binding. ImageJ software was used to measure the dot densities of the scanned blot images

Vascular endothelial growth factor and IL8 enzyme-linked immunosorbent assay. HCT116 control vector–transfected and PPARD vector–transfected cells were cultured in serum-free medium for 48 h, and the culture media (conditioned media) were then separately collected. Vascular endothelial growth factor and IL8 levels in culture supernatants from HCT116 control vector–transfected and PPARD vector-transfected cells were examined using a human vascular endothelial growth factor or IL8 specific Quantikine enzyme-linked immunosorbent assay kit (R&D Systems) according to the manufacturer's instructions.

Tubule formation assay. 1) HCT116 control vector-transfected and PPARD vector-transfected HCT116 cells were grown separately in RPMI medium with no FBS supplementation for 48 h; 2) HCT116 WT cells were treated with the PPARD agonist GW0742 (1 μM) or control solvent dimethyl sulfoxide for 48 h; and 3) HCT116 control vector-transfected and PPARD vector-transfected HCT116 cells were treated with an anti-IL8 antibody (1 μg/mL, catalog #MAB208, R&D Systems) or control immunoglobulin G for 72 h. Then, the media were collected and mixed with equal volumes of fresh RPMI medium supplemented with 2% FBS to generate 3 conditioned media (control vector and PPARD vector) with final concentrations of 1% FBS. For the tubule formation assay(9), 12-well plates were coated with 500 μL of an equal mixture of growth factor-reduced Matrigel and serum-free RPMI medium and incubated for 15 min at 37°C. Cells (1×10^5) were resuspended in 500 μL of appropriately conditioned medium, dispensed onto growth factor-reduced Matrigel-coated wells, and incubated for 12 h. Tubules were quantified by counting all connecting branches between discrete endothelial cells in 3 random fields from each well at 100× magnification. Each experiment used medium supplemented with 1% FBS as a negative control and HUVEC culture medium as a positive control.

Analysis of IL8 promoter activity. To determine whether PPARD regulates IL8 expression through a transcriptional mechanism, HCT116 and HCT116-PPARD-KO cells or LoVo cells transiently transfected with PPARD expression vector or control vector were transiently cotransfected with IL8 promoter luciferase constructs (-1481 to +50 bp [-1481], -546 to +50 bp [-546], -276 to +50 bp [-276], and -133 to +50 bp [-133]) and the pSV-β-galactosidase vector

(Promega) using Lipofectamine 2000 (Invitrogen). The luciferase activity was measured 24 h after transfection as described previously(1).

Chromatin immunoprecipitation-quantitative polymerase chain reaction assay. To determine whether PPARD binds to a target gene (interleukin [IL]-8 or GJA1) promoter, we subjected HCT116 WT, PPARD-KO, and PPARD-KO-PD cells to chromatin immunoprecipitation (ChIP). The cells were cross-linked by adding formaldehyde to the culture medium to a final concentration of 1% and incubating the medium for 10 min at 37°C. ChIP assays were performed using EpiTect ChIP OneDay kit according to the manufacturer's protocol (Qiagen, catalog #334471). Chromatin was immunoprecipitated using a specific anti-human PPARD antibody (Santa Cruz Biotechnologies, sc-7197×). The following primers were used to amplify a 113-bp fragment of the IL8 promoter: 5'-CATCAGTTGCAAATCGTGGA-3' (sense) and 5'- TTTGTGCCTTATGGAGTGCT-3' (antisense). IL8 luciferase deletion promoter assays revealed the amplified IL8 promoter sequence fragment to be in the region of -276 to -133 bp of the IL8 promoter. Primers from Qiagen (ChIP quantitative polymerase chain reaction [qPCR] Primer Assay For Human GJA1, NM_000165.3 [-]01Kb, ChIP-qPCR Assay catalog #GPH1011562[-]01A) were used to amplify a 107-bp fragment of the GJA1 promoter, which was just next to a PPAR binding sequence, AACAGGTCACTCACACCTACCT, upstream of the GJA1 promoter, as identified via the Champion ChIP Transcription Factor Search Portal, which is based on SABiosciences' proprietary database, DECipherment Of DNA Elements. Primers from Qiagen (ChIP-qPCR Human IGX1A Negative Control; catalog #GPH100001C[-]01A) were used as ChIP-qPCR nonspecific negative controls. QPCR was performed using SYBR Green ROX qPCR Mastermix (Qiagen, catalog #330520) with amplification conditions as

follows: 95°C for 10 min and then 95°C for 15 s and 60°C for 1 min for 40 cycles. To assess the relative binding of PPARD to the IL8 or GJA1 promoter region, we used the comparative C_t method to calculate the relative sequence abundance of the ChIP DNA fraction to the input sample (% input) according to the following formula: % input = $[2^{Ct(input)-Ct(ChIP)}] \times 100$. The C_t value of the ChIP DNA sample is donated by Ct (ChIP), and that of the input is donated by Ct (input)(10).

Migration and invasion assay. Migration and invasion assays were performed as described previously(11). For the migration assay, equal numbers of cells were plated on the tops of the well inserts, and 0.75 mL of the same medium was added to the bottoms of the wells. After 48 h of incubation, cells that had not migrated were scraped from the top compartment, and cells that had migrated through the membrane were fixed and stained using the protocol of the HEMA 3 stain set (Thermo Fisher Scientific). Membranes were excised and mounted on a standard microscope slide (Curtin Matheson Scientific). The migrated cells in at least 4 random individual high-power fields per insert membrane were photographed with a light microscope at magnification ×200 and then counted. The invasion assay was similar to the migration assay, except the cells in the invasion assay were placed in the top insert, and the insert membrane was coated with 100 μL of growth factor-reduced Matrigel diluted to 300 μg protein/mL (BD Biosciences).

Soft agar colony-forming assay. To determine the effect of PPARD expression on anchorage-independent cell growth, we coated 6-well plates with 2 mL of medium with 0.6% Noble agar per well and added 1000 B16-F10 cells stably transfected with control-shRNA or PPARD-

shRNA (PPARD-shRNA-A-clone1 or -clone2) in 1 mL of medium containing 0.33% agarose to the wells. After the 0.33% agarose solidified, 1 mL of 10% FBS of DMEM medium was added. Cells were incubated for 18 days. Colonies were stained with 100 μL of a 5 mg/mL solution of 3-(4,5-dimethylthiazol-2-yl)-2,5-diphenyltetrazolium bromide/well at 37°C for 2 h and then photographed.

PPARD immunohistochemical staining. Immunohistochemical staining for PPARD was performed as described previously (3) using an antibody against human PPARD (Abcam, ab23673, 1:100) on 5 tissue microarray slides containing colectomy samples from 152 colorectal cancer patients. The staining results were scored on the basis of the percentage of tumor cells with nucleic or cytoplasmic staining (<10%, 0; 10% to <25%, 1; 25% to <50%, 2; 50% to <75%, 3; and >75%, 4) and staining intensity (no staining, 0; light brown, 1; brown, 2; and dark brown, 3). Composite expression scores were calculated as 4×(intensity-1) + frequency(12) .

SUPPLEMENTAL METHODS REFERENCES

1. Shureiqi I, Jiang W, Zuo X, Wu Y, Stimmel JB, Leesnitzer LM, Morris JS, Fan HZ, Fischer SM, and Lippman SM. The 15-lipoxygenase-1 product 13-S-hydroxyoctadecadienoic acid down-regulates PPAR-delta to induce apoptosis in colorectal cancer cells. *Proc Natl Acad Sci U S A.* 2003;100(17):9968-73.
2. Gray MJ, Van Buren G, Dallas NA, Xia L, Wang X, Yang AD, Somcio RJ, Lin YG, Lim S, Fan F, et al. Therapeutic targeting of neuropilin-2 on colorectal carcinoma cells implanted in the murine liver. *J Natl Cancer Inst.* 2008;100(2):109-20.
3. Shureiqi I, Wu Y, Chen D, Yang XL, Guan B, Morris JS, Yang P, Newman RA, Broaddus R, Hamilton SR, et al. The critical role of 15-lipoxygenase-1 in colorectal epithelial cell terminal differentiation and tumorigenesis. *Cancer Res.* 2005;65(24):11486-92.
4. Pfaffl MW. A new mathematical model for relative quantification in real-time RT-PCR. *Nucleic Acids Res.* 2001;29(9):e45.
5. Merritt WM, Lin YG, Spannuth WA, Fletcher MS, Kamat AA, Han LY, Landen CN, Jennings N, De Geest K, Langley RR, et al. Effect of interleukin-8 gene silencing with liposome-encapsulated small interfering RNA on ovarian cancer cell growth. *J Natl Cancer Inst.* 2008;100(5):359-72.
6. Kim TJ, Ravoori M, Landen CN, Kamat AA, Han LY, Lu C, Lin YG, Merritt WM, Jennings N, Spannuth WA, et al. Antitumor and antivascular effects of AVE8062 in ovarian carcinoma. *Cancer Res.* 2007;67(19):9337-45.
7. Lee JW, Han HD, Shahzad MM, Kim SW, Mangala LS, Nick AM, Lu C, Langley RR, Schmandt R, Kim HS, et al. EphA2 immunoconjugate as molecularly targeted chemotherapy for ovarian carcinoma. *J Natl Cancer Inst.* 2009;101(17):1193-205.
8. Thaker PH, Han LY, Kamat AA, Arevalo JM, Takahashi R, Lu C, Jennings NB, Armaiz-Pena G, Bankson JA, Ravoori M, et al. Chronic stress promotes tumor growth and angiogenesis in a mouse model of ovarian carcinoma. *Nat Med.* 2006;12(8):939-44.
9. Ito Y, Oike Y, Yasunaga K, Hamada K, Miyata K, Matsumoto S, Sugano S, Tanihara H, Masuho Y, and Suda T. Inhibition of angiogenesis and vascular leakiness by angiopoietin-related protein 4. *Cancer Res.* 2003;63(20):6651-7.
10. Zuo X, Shen L, Issa JP, Moy O, Morris JS, Lippman SM, and Shureiqi I. 15-Lipoxygenase-1 transcriptional silencing by DNA methyltransferase-1 independently of DNA methylation. *Faseb j.* 2008;22(6):1981-92.
11. Wu Y, Mao F, Zuo X, Moussalli MJ, Elias E, Xu W, and Shureiqi I. 15-LOX-1 suppression of hypoxia-induced metastatic phenotype and HIF-1alpha expression in human colon cancer cells. *Cancer Med.* 2014;3(3):472-84.
12. Soutto M, Belkhiri A, Piazuelo MB, Schneider BG, Peng D, Jiang A, Washington MK, Kokoye Y, Crowe SE, Zaika A, et al. Loss of TFF1 is associated with activation of NF-kappaB-mediated inflammation and gastric neoplasia in mice and humans. *J Clin Invest.* 2011;121(5):1753-67.

Supplemental Table 1. Clinical Characteristics of the Study Sample of 22 Patients with Stage III Colorectal Cancer

Case No.	Age, Years *	Sex	Disease Site	Disease Stage	Metastatic Disease	Disease-Free Interval, Months†	Neoadjuvant and Adjuvant Chemotherapy	Metastasis Site(s)
1	57	M	Rectosigmoid colon	IIIb	Yes	8.7	Neoadjuvant chemoradiation with capecitabine and postoperative adjuvant capecitabine	Liver and lung
2	53	M	Cecum	IIIb	Yes	15.2	No adjuvant chemotherapy‡	Peritoneum and lymph nodes
3	63	M	Sigmoid colon	IIIb	Yes	9.7	Adjuvant capecitabine	Liver, peritoneum, and lung
4	49	F	Ascending colon	IIIb	Yes	8.9	Adjuvant capecitabine	Lung
5	43	M	Ascending colon	IIIc	Yes	7.5	Adjuvant FOLFOX	Liver, peritoneum, and lymph nodes
6	65	F	Ascending colon	IIIb	Yes	30.2	Adjuvant FOLFOX	Lymph node
7	53	F	Ascending colon	IIIc	Yes	14.4	Adjuvant irinotecan, 5-fluorouracil, and leucovorin	Peritoneum and abdominal wall
8	66	F	Rectum	IIIc	Yes	16.9	Neoadjuvant chemoradiation with capecitabine and postoperative adjuvant FOLFOX	Lung and peritoneum
9	60	M	Rectum	IIIb	Yes	24.7	Neoadjuvant chemoradiation with capecitabine and postoperative adjuvant FOLFOX	Pelvic soft tissue and peritoneum
10	54	F	Rectum	IIIb	Yes	11.5	Neoadjuvant chemoradiation with capecitabine**	Pelvis and lung
11	54	F	Hepatic flexure	IIIc	No	80.1	Adjuvant FOLFOX, then later irinotecan and oxaliplatin††	None
12	79	F	Ascending colon	IIIc	No	48.9	Adjuvant FOLFOX	None
13	65	M	Descending colon	IIIb	No	47	Adjuvant FOLFOX	None
14	29	F	Cecum	IIIb	No	115	Adjuvant FOLFOX	None
15	45	F	Descending colon	IIIb	No	55.8	Adjuvant capecitabine and oxaliplatin	None
16	59	M	Cecum and transverse colon	IIIb	No	41	Adjuvant FOLFOX	None
17	60	F	Cecum	IIIc	No	54.8	Adjuvant capecitabine	None
18	57	M	Ascending colon	IIIb	No	86.2	Adjuvant FOLFOX	None
19	48	M	Sigmoid colon	IIIb	No	68.4	Adjuvant FOLFOX	None
20	53	F	Transverse colon	IIIb	No	64.7	Adjuvant FOLFOX and bevacizumab	None
21	63	M	Splenic flexure	IIIc	No	55.7	Adjuvant FOLFOX	None
22	67	F	Rectosigmoid colon	IIIb	No	48.8	Adjuvant FOLFOX, then later capecitabine and oxaliplatin	None

FOLFOX indicates oxaliplatin, 5-fluorouracil, and leucovorin.

*Age at the time of primary colorectal cancer resection.

†Time between resection and development of metastatic disease or last follow-up (if no metastasis).

‡No adjuvant chemotherapy was given owing to comorbidities (renal failure, heart disease, and hepatitis C virus infection).

**No postoperative adjuvant therapy was given because of dihydropyrimidine dehydrogenase deficiency.

††Adjuvant therapy was switched because the patient developed chest pain.

Supplemental Table 2. Genes Differentially Upregulated in Transcriptome Analysis of HCT-116 Cells with and without PPARD Knockout (KO) That Have Significant Association with PPARD Expression in The Cancer Genome Atlas (TCGA) Provisional Colorectal Cancer Database

Gene	Transcriptome Analysis in HCT-116-WT and HCT-116-PPARD-KO Cells			Association with PPARD mRNA in TCGA Database	
	Ratio of RNA Expression Levels*	P value	Q value	Log Odds Ratio	P value
GJA1	874.4552140	1.00E-300	5.38E-299	2.228	0.036
HCLS1	60.14489223	1.00E-300	5.38E-299	2.197	0.011
VIM	32.69811046	1.00E-300	5.38E-299	1.645	0.038
SPARC	30.01299596	1.00E-300	5.38E-299	1.770	0.028
ALPK2	28.99010151	1.15E-69	6.70E-69	2.720	0.004
LSP1	13.97250476	1.43E-160	2.74E-159	2.159	0.004
NRG1	13.64857721	1.93E-156	3.60E-155	1.709	0.033
CXCL8 (IL8)	9.318424135	1.00E-300	5.38E-299	2.070	0.045
ALPL	7.863069600	1.73E-52	7.28E-52	2.413	0.027
SLC26A9	6.161721437	1.55E-44	5.26E-44	1.776	0.028
C11ORF86	5.603304602	2.77E-42	8.86E-42	>3	0.008
P2RX7	5.321928625	8.87E-30	1.92E-29	1.849	0.024
FBXO32	4.691060547	3.95E-53	1.68E-52	1.785	0.006
RCN3	4.588546648	5.86E-19	7.67E-19	2.009	0.017
ALDH1L2	4.450206428	1.67E-46	5.95E-46	1.709	0.033
STC1	4.142106451	7.76E-34	1.93E-33	1.911	0.009
FRMD4B	4.134879644	6.82E-94	5.94E-93	2.426	0.007
GFPT2	3.962814536	4.33E-106	4.47E-105	2.092	0.005
SEPP1	3.513287151	9.56E-32	2.21E-31	2.197	0.011
SYNE1	3.425668913	1.71E-84	1.25E-83	2.482	0.002
CDKN2B	3.337533012	1.60E-132	2.32E-131	2.009	0.017
SNCG	3.274848126	1.97E-100	1.90E-99	2.099	0.014
RNF144B	3.205067774	7.88E-22	1.21E-21	2.930	0.014

*HCT-116-WT cells vs. HCT-116-PPARD-KO cells.

Supplemental Table 3. Clinical Characteristics of the Study Sample of 152 Patients with Stage II-IV Colorectal Cancer

No. of Patients	Disease Stage	Mean Age ± SD, Years	Mean Metastasis-Free Survival Duration ± SD, Days	Neoadjuvant and Adjuvant Chemotherapy (% of Patients)	Primary Disease Site (% of Patients)
71	II	65.41 ± 11.31	2248.07 ± 1101.17	Fluoropyrimidine (23) Oxaliplatin + fluoropyrimidine (7) No adjuvant chemotherapy (65) Adjuvant chemotherapy was received at an outside institution without further details (1) Unknown whether adjuvant chemotherapy was given (4)	Right colon (45) Left colon (55)*
70	III	61.78 ± 13.43	2055.83 ± 1154.02	Oxaliplatin + fluoropyrimidine (64) Fluoropyrimidine only (17) Irinotecan + fluoropyrimidine (4) No adjuvant chemotherapy (14)	Right colon (52) Left colon (48)
11	IV	61.60 ± 15.21	N/A	N/A	Right colon (27) Left colon (73)

SD indicates standard deviation.

*One patient had synchronous left and right colon cancers.

Supplemental Table 4. Prognostic Impact of PPARD Expression on Tumor-Specific Event–Related Survival in Publicly Available Cancer Microarray Datasets in the PrognoScan Database*

Dataset	Cancer Type	Endpoint	Cohort	Array Type	Probe ID	No. of Patients	Cut-point	Minimum P Value	Corrected P Value	$\ln(HR_{high}/HR_{low})$	Cox P Value	ln(HR)	HR (95% CI)
GSE3494-GPL96	Breast cancer	Disease-specific survival	Uppsala (1987-1989)	HG-U133A	37152_at	236	0.63	0.00146	0.034963	0.84	0.00518	1.07	2.93 (1.38-6.22)
GSE2034	Breast cancer	Distant metastasis–free survival	Rotterdam (1980-1995)	HG-U133A	37152_at	286	0.87	0.00013	0.004437	0.88	0.00149	0.68	1.98 (1.30-3.03)
GSE11121	Breast cancer	Distant metastasis–free survival	Mainz (1988-1998)	HG-U133A	37152_at	200	0.54	0.00196	0.044458	0.94	0.01999	0.99	2.69 (1.17-6.20)
GSE30929	Soft tissue cancer (liposarcoma)	Distant recurrence–free survival	MSKCC (1993-2008)	HG-U133A	37152_at	140	0.76	0.00103	0.026157	0.95	0.05022	0.85	2.35 (1.00-5.51)
GSE1378	Breast cancer	Relapse-free survival	MGH (1987-2000)	Arcturus 22k	7260	60	0.88	0.00001	0.000409	1.88	0.00027	0.71	2.02 (1.39-2.96)
GSE31210	Lung cancer (adenocarcinoma)	Relapse-free survival	NCCRI (1998-2008)	HG-U133_Plus_2	37152_at	204	0.78	0.00022	0.006886	0.99	0.01372	0.89	2.45 (1.20-4.98)
GSE1379	Breast cancer	Relapse-free survival	MGH (1987-2000)	Arcturus 22k	7260	60	0.62	0.00177	0.040917	1.14	0.02543	0.84	2.32 (1.11-4.85)

HR indicates hazard ratio; CI, confidence interval; MSKCC, Memorial Sloan Kettering Cancer Center; MGH, Massachusetts General Hospital; NCCRI, National Cancer Center Research Institute (Japan).

*Studies were identified in a search performed December 17, 2014.